Density Functional Theory Study of Transition-Metal Compounds Containing Metal−Metal Bonds. 2. Molecular Structures and Vibrational Spectra of Dinuclear Tetracarboxylate Compounds of Molybdenum and Rhodium

F. Albert Cotton* and Xuejun Feng*

Contribution from the Department of Chemistry and Laboratory for Molecular Structure and Bonding, Texas A&M University, College Station, Texas 77843-3255

Received November 6, 1997

Abstract: Vibrational spectra have been calculated for the first time for dinuclear transition-metal compounds containing metal−metal bonds. The calculations were carried out by employing different forms of density functional theory (DFT) and basis functions of different sizes at fully optimized molecular geometry. The calculated frequencies essentially reproduced fundamentals observed in experimental infrared and Raman spectra. It is shown that DFT frequency calculations can be a very important and valuable tool to assist in analyzing and assigning measured infrared and Raman spectra and to predict vibrational frequencies for large transition-metal compounds with metal−metal bonds. The molecules included in this study were $M_2(O_2CH)_4$ (M = Mo, Rh), $Rh_2(O_2CH)_4(H_2O)_2$, and $M_2(O_2CCH_3)_4$ (M = Mo, Rh). Significant differences are found between the formate and acetate molecules.

Introduction

Transition-metal compounds containing metal-to-metal bonds[1] are known to pose challenges to quantum chemical computations of their electronic and structural properties. In addition to their relatively large molecular size, electron correlation effects associated with metal-to-metal bonding are exceptionally strong so that an accurate calculation of these properties can be difficult or simply impractical with more traditional ab initio methods.[2] Recent developments in density functional theory (DFT)[3] have shown that DFT may become a powerful computational alternative to the conventional quantum chemical methods. DFT calculations are much less computationally demanding, yet take account of the effects of electron correlation. These methods, therefore, may be particularly suitable for treating the compounds with metal−metal bonds.

In this laboratory, we have been exploring the application of DFT methods to the study of electronic and structural properties of the metal−metal-bonded systems. In the first paper[2] (part one, hereafter) of a series we plan to publish, we have shown that molecular structures of many crystallographically characterized compounds of the second-row metals with metal−metal bonds of various orders can be accurately reproduced by complete geometry optimization using DFT methods. Notably, the structural parameters predicted from these calculations for a niobium compound with a metal−metal triple bond before it was made have been nicely confirmed very recently by X-ray crystallographic data on a very similar compound.[4] Encouraged by the success in the DFT calculations of molecular structures, we continue our exploration by applying DFT methods to those molecular properties that are closely related to molecular structure. We report in this second paper of the series density functional calculations of vibrational frequencies for metal−metal-bonded compounds.

Vibrational spectra and, in particular, metal−metal stretching vibrations have been of great interest among various spectroscopic properties of the metal complexes containing metal−metal bonds.[1] Infrared (IR) and Raman spectra of many these compounds have been recorded in efforts to determine the metal−metal stretching vibration frequencies and, therefore, to elucidate the nature of the metal−metal bonding.[1] The measurements usually give rise to complicated spectra, which is apparently associated with the complex molecular structures (e.g., fused heterocyclic rings) of these large systems, so that assignments of the measured spectra very often are not an easy task and are not without controversy. In such a situation, accurate theoretical calculations of vibrational frequencies become desirable and can be expected to afford invaluable assistance in assigning the measured spectra. Such calculations can also be particularly valuable in cases when experimental measurements are difficult to carry out for various reasons.

DFT methods are known to offer promise of obtaining accurate vibrational frequencies[5] and, in fact, have already been used in the study of vibrational spectra of a variety of molecular systems including transition-metal complexes.[6] Little was yet known, however, about the applicability of the DFT methods

(1) Cotton, F. A.; Walton, R. A. *Multiple Bonds between Metal Atoms*, 2nd ed.; Oxford University Press: Oxford, U.K., 1992.

(2) Cotton, F. A.; Feng, X. *J. Am. Chem. Soc.* **1997**, *119*, 7514.

(3) (a) Parr, R. G.; Yang, W. *Density Functional Theory of Atoms and Molecules*; Oxford University Press: Oxford, 1989. (b) Seminario, J. M.; Politzer, P. *Modern Density Functional Theory, A Tool for Chemistry*; Elsevier Science B.V.: Amsterdam, The Netherlands, 1995.

(4) Cotton, F. A.; Matonic, J. H.; Murillo, C. A. *J. Am. Chem. Soc.* **1997**, *119*, 7889.

(5) Johnson, B. G.; Gill, P. M. W.; Pople, J. A. *J. Chem. Phys.* **1993**, *98*, 5612.

(6) See, for example: (a) Berces, A.; Ziegler, T. *J. Phys. Chem.* **1994**, *98*, 13233. (b) Berces, A.; Ziegler, T.; Fan, L. *J. Phys. Chem.* **1994**, *98*, 1584. (c) Berces, A.; Ziegler, T. *J. Chem. Phys.* **1993**, *98*, 4793.

S0002-7863(97)03823-7 CCC: $15.00
Published on Web 03/26/1998

Table 1. Calculated Structural Parameters with Comparison to Crystal Structure Data for $Mo_2(O_2CH)_4$

	3-21G					LARGE					
	SVWN	BLYP[a]	BPW91	B3LYP[a]	B3PW91	SVWN	BLYP	BPW91	B3LYP	B3PW91	exptl[b]
						distance (Å)					
Mo−Mo	2.111	2.142	2.125	2.108	2.096	2.138	2.168	2.149	2.129	2.114	2.091(2)
Mo−O	2.051	2.122	2.105	2.107	2.094	2.075	2.149	2.132	2.135	2.122	2.109(13)
O−C	1.295	1.313	1.309	1.295	1.293	1.293	1.311	1.306	1.294	1.291	1.29(2)
C−H	1.098	1.096	1.095	1.087	1.088	1.093	1.095	1.094	1.087	1.087	0.97
						angle (deg)					
Mo−Mo−O	92.05	92.10	92.28	92.11	92.25	91.58	91.67	91.84	91.75	91.90	92.0(4)
Mo−O−C	117.25	116.84	116.59	117.02	116.87	117.78	117.29	117.10	117.45	117.28	117(1)
O−Mo−O	89.93	89.92	89.91	89.92	89.91	89.96	89.95	89.94	89.95	89.94	90.0(5)
H−C−O	119.30	118.93	118.87	119.13	119.12	119.37	118.97	118.95	119.21	119.18	119

[a] From previous work (see ref 2). [b] Average bond distances and angles from crystal structure data of $Mo_2(O_2CH)_4$ (see ref 13).

Table 2. Results of Geometry Optimization for the Formate Compounds $Rh_2(O_2CH)_4$ and $Rh_2(O_2CH)_4(H_2O)_2$

	$Rh_2(O_2CH)_4$				$Rh_2(O_2CH)_4(H_2O)_2$			
	3-21G		LARGE		3-21G	LARGE		
	B3LYP	B3PW91	B3LYP	B3PW91	B3PW91	B3LYP	B3PW91	exptl[a]
					distance (Å)			
Rh−Rh	2.400	2.383	2.426	2.407	2.410	2.454	2.436	2.3855(5)
Rh−O	2.063	2.050	2.085	2.071	2.053 2.063	2.088 2.100	2.074 2.084	2.039(8)
O−C	1.290	1.288	1.290	1.287	1.292 1.282	1.292 1.285	1.289 1.282	1.269(4)
Rh−OH_2					2.296	2.318	2.301	2.310(3)
					angle (deg)			
Rh−Rh−O	88.67	88.85	88.30	88.50	89.49 87.52	88.85 87.06	89.00 87.25	88.07(26)
Rh−O−C	118.09	117.87	118.48	118.28	117.16 118.93	117.89 119.38	117.67 119.18	119.50(30)
O−C−O	126.47	126.56	126.44	126.44	126.89	126.82	126.89	124.8(3)
Rh−Rh−OH_2					169.42	173.70	174.14	176.47(6)

[a] Average bond distances and angles from crystal structure data of $Rh_2(O_2CCH_3)_4(H_2O)_2$ (see reference 12).

to the metal−metal-bonded systems in this regard. In addition, to the best of our knowledge, there have not been any reported ab initio or other calculations on vibrational spectra for the metal−metal-bonded species by quantum chemical methods, except for the few cases in which the metal−metal stretching frequencies and associated force constants were calculated.[7]

In the present paper, we report the results of DFT calculations on vibrational spectra and molecular structures for a number of dinuclear tetracarboxylate compounds of molybdenum and rhodium, namely, $M_2(O_2CH)_4$ (M = Mo, Rh), $Rh_2(O_2CH)_4(H_2O)_2$, and $M_2(O_2CCH_3)_4$ (M = Mo, Rh). We have chosen the dimolybdenum compounds for the present study because of their special and central role as the best known quadruply bonded species in the study of metal−metal bonding in addition to their well-characterized structures and the abundant spectroscopic data.[1] On the other hand, the vibrational spectra of the singly bonded dirhodium compounds have been of special interest because of earlier controversy concerning assignment of Rh−Rh stretching vibrations in early studies.[1]

As we will see, in addition to a correct prediction of the metal−metal stretching frequencies, we can actually calculate the full spectrum of fundamental frequencies for all molecular vibrations in the dinuclear compounds with metal−metal bonds.

Computational Procedures

The DFT calculations on harmonic vibrational frequencies were performed by utilizing fully optimized molecular geometry as the reference geometry.

The DFT geometry optimization was carried out for $Mo_2(O_2CH)_4$ with (1) the local spin density approximation using Slater exchange and Vosko−Wilk−Nusair correlation functional[8a] (SVWN), (2) the Becke−Lee−Yang−Parr (BLYP)[8b,c] and Becke−Perdew−Wang (BPW91)[8c,d] gradient-corrected density functional methods, and (3) the hybrid functional[8e] B3LYP and B3PW91 methods. For all other molecules, only the B3LYP and B3PW91 methods were used in geometry optimization, since these two functionals have been shown to afford the best optimized molecular structures both in our previous study[2] and in the present one. For the same reason, the B3LYP and B3PW91 methods were used in frequency calculations for all dinuclear compounds.

Two types of basis functions were employed in both geometry optimization and frequency calculations. The first type includes the limited 3-21G basis sets for both metal atoms and all other main group elements. In the second type of basis sets, the 6-31G sets were used for all main group atoms, and a [10s6p5d] contraction of the (17s11p8d) primitive set by Huzinaga[9] was employed for the metal atoms using a segmented contraction scheme. The metal basis set was further augmented by adding two diffuse p functions of exponents 0.1496 and 0.062 for Mo and 0.20 and 0.09 for Rh, which leads to a full double-ζ basis set with triple-ζ for valence d functions. This second type of basis set will be referred to as LARGE in the following discussion. It may be pointed out that the LARGE basis set in the present case is different from the basis set of the same label in part one in that in the previous case the metal basis functions were contracted to valence double-ζ only.

The molecular symmetry used in the calculations is as follows, namely, D_{4h} for the formate compounds $M_2(O_2CH)_4$ (M = Mo, Rh), C_{2h} for $Rh_2(O_2CH)_4(H_2O)_2$, and C_{4h} for the acetate compounds $M_2(O_2CCH_3)_4$.

All calculations were carried out by using the Gaussian 94 program[10] and were performed on SGI Power Challenge computers.

(7) Ziegler, T. *J. Am. Chem. Soc.* **1985,** *107*, 4453.
(8) (a) Vosko, S. H.; Wilk, L.; Nusair, M. *Can. J. Phys.* **1980**, *58*, 1200. (b) Becke, A. D. *Phys. Rev. A* **1988**, *38*, 3098. (c) Lee, C.; Yang, W.; Parr, R. G. *Phys. Rev. B* **1988**, *37*, 785. (d) Perdew, J. P.; Wang, Y. *Phys. Rev.* **1992**, *B45*, 13244. (e) Becke, A. D. *J. Chem. Phys.* **1993**, *98*, 5648.
(9) Huzinaga, S. *J. Chem. Phys.* **1977**, *66*, 4245.
(10) Frisch, M. J.; Frisch, A. E.; Foresman, J. B. *Gaussian 94 User's Reference*; Gaussian Inc.: Carnegie Office Park, Building 6, Pittsburgh, PA 15106.

Results and Discussion

A. The Formate Compounds. Molecular Structures. The reference geometries for our vibrational frequency calculations are the ones that were fully optimized by the same DFT methods. Shown in Tables 1 and 2 are the structural parameters of the optimized geometry for the dimolybdenum and dirhodium formate compounds, respectively.

We have shown in part one that the molecular structure of $Mo_2(O_2CH)_4$ can be precisely reproduced by the B3LYP method even with the limited 3-21G basis sets. Table 1 includes the results of the earlier calculations and those from the present work by using the SVWN, BPW91, and B3PW91 methods and a different LARGE basis set. It is clear from Table 1 that very similar conclusions to those reached previously in part one can be drawn. We see again that the results of different DFT calculations are all in an excellent agreement with the experimental values, but the hybrid B3LYP and B3PW91 methods are obviously superior to the pure DFT methods in geometry optimization. In addition, it is noted that the B3PW91 bond lengths are always a little shorter than the corresponding B3LYP distances and are closer to those from crystal structure data. Such discrepancies become more pronounced in the dirhodium compounds in which the metal−metal bond is much weaker, as we will see shortly. Again, as noted before, for a given DFT method, the values of the Mo−Mo distance and many other bond parameters calculated with the 3-21G basis set are always in slightly better agreement with the measured data.

The bond distances from the SVWN calculations require special comment. The calculated Mo−O distance in this case is notably shorter than those obtained by any of the other methods and that obtained from experiment. One might attribute the shortness to overbinding of the Mo−O bond associated with the local spin density approximation.[11] The O−C distance so calculated, on the other hand, appears to be normal when compared with the results by other methods and agrees well with the crystal structure data. It is interesting and important to note that the SVWN method makes excellent metal−metal distance predictions which are superior to those by the BLYP and BPW91 methods and are only slightly longer than those produced by the hybrid methods.

The optimized molecular structures for $Rh_2(O_2CH)_4$ and $Rh_2(O_2CH)_4(H_2O)_2$ are given in Table 2. Unfortunately, there are no reliable experimental structural data for either one. Moreover, there is no $Rh_2(O_2CR)_4$ compound known in the solid state that does not have axial ligation, either with additional donor molecules, as in $Rh_2(O_2CR)_4L_2$ compounds, or because the $Rh_2(O_2CR)_4$ molecules form infinite chains in which one oxygen atom at each end of the dinuclear $Rh_2(O_2CR)_4$ molecule serves as an axial ligand to an adjacent molecule. For these reasons, we have compared the computational results with experimental data for $Rh_2(O_2CCH_3)_4(H_2O)_2$ in Table 2. The calculated results for the $Rh_2(O_2CH)_4$ and $Rh_2(O_2CH)_4(H_2O)_2$ molecules are interesting because they show, consistently for each type of calculation, that the effect of introducing the axial water molecules is to lengthen the Rh−Rh bond, as expected, but only by a small amount (namely, about 0.03 Å).

Vibrational Spectrum of $Mo_2(O_2CH)_4$. The calculated vibrational frequencies for $Mo_2(O_2CH)_4$ are shown in Table 3 together with the experimental values from infrared (IR) and Raman (R) spectroscopic measurements. The table includes frequencies given by the B3LYP and B3PW91 calculations in both 3-21G and LARGE basis sets. Also listed are the symmetry labels of the normal modes of vibration and a description of each normal mode based on the calculated nuclear displacements corresponding to that mode. Two sets of experimental data are listed for comparison, namely, Raman data by Cotton et al.[13] and IR/Raman data with assignments by Akhmedov et al.[14]

As shown in Table 3, the calculated frequencies by the two different DFT methods in a given basis set are very similar. Sightly larger differences can be seen in the stretching frequencies, which may be traced to differences in the optimized molecular structures. Higher B3PW91 frequencies correspond to shorter bond distances in the B3PW91 geometry. It is very interesting and also important to note that there are no significant differences between the results calculated by using the limited 3-21G basis set and those obtained by employing the much extended LARGE basis set for this molecule and other molecules considered in this work. A notable difference is the higher frequencies for the Mo−Mo and Mo−O stretching vibrations given by the 3-21G basis set, which again may be related to the shorter bond lengths in the 3-21G geometry. Because of these quantitatively similar results, we will proceed in the following discussion by considering only one set, namely, the results from the B3PW91 calculation in the LARGE basis set (bold-faced column in Table 3).

We have given in Table 3 a simple description for each normal mode of vibration according to the calculated nuclear displacements associated with that mode. Our calculations show that in only a vary few cases may a normal mode be associated with a single type of localized vibrational motion. Figure 1 shows two such examples, namely, an a_{1u} mode at 180 cm^{-1} for Mo−Mo torsion only and a b_{1u} mode at 283 cm^{-1} for O−Mo−O bending only. In most cases, coupling of different vibrational motions is extensive for a given mode. The simple description for a normal mode, therefore, may reflect only the principal contribution to the actual molecular vibration. Examples are the coupling of the Mo−Mo and Mo−O stretching vibrations as illustrated in Figure 2 by two a_{1g} normal modes. In Figures 1 and 2 as well as in other similar figures we will introduce later, the length of an arrow that points away from a nuclear position represents the relative displacement of that vibrating atom from its equilibrium position. It may be mentioned that extensive couplings are common and very similar in molecular vibrations of all compounds studied in this work.

There are all together 48 normal modes of vibration for the $Mo_2(O_2CH)_4$ molecule. For such a molecule in D_{4h} symmetry, all normal modes of g symmetry are, as always with inversion symmetry, Raman-active only and all those of u symmetry are IR-active only, except for the modes of a_{2g}, a_{1u}, b_{1u}, and b_{2u} symmetries which are neither Raman- nor IR-active.[15] We have taken these selection rules into consideration when comparing the calculated frequencies to the measured spectra in Table 3. However, as can be seen in Table 3 and also known in other cases,[15] the symmetry requirements may not be always satisfied in the study of real spectra of complicated molecular systems. For the sake of convenience in the following discussion, we have divided the calculated frequencies into blocks in Table 3 and in all other tables to be discussed later. Each of these blocks corresponds to the normal modes of a given type of vibration.

(11) Ziegler, T. *Chem. Rev.* **1991**, *91*, 651.

(12) Cotton, F. A.; DeBoer, B. G.; LaPrade, M. D.; Pipal, J. R.; Ucko, D. A. *Acta Crystallogr.* **1971**, *B27*, 1664.

(13) Cotton, F. A.; Norman, J. G., Jr.; Stults, B. R.; Webb, T. R. *J. Coord. Chem.* **1976**, *5*, 217.

(14) Akhmedov, E. L.; Kotel'nikova, A. S.; Evstaf'eva, O. N.; Kharitonov, Yu. Ya.; Smirnov, A. N.; Tsivadze, A. Yu.; Babievskaya, I. Z.; Abbasov, A. M. *Sov. J. Coord. Chem.* **1987**, *13*, 273.

(15) Clark, R. J. H.; Hempleman, A. J.; Kurmoo, M. *J. Chem. Soc., Dalton Trans.* **1988**, 973.

Table 3. Calculated Vibrational Frequencies (cm^{-1}) for $Mo_2(O_2CH)_4$ with Comparison to Experimental Measurements

		3-21G		LARGE		exptl		
sym	normal modes	B3LYP	B3PW91	B3LYP	B3PW91	R[a]	IR/R[b]	assignment
						84 95		
e_u	O−Mo−O bending	123	125	123	**123**	132		
b_{2g}	out-of-plane CH rocking	128	131	128	**129**	147		
a_{1u}	Mo−Mo torsion	177	179	179	**180**			
b_{2u}	in-plane C−H/O−C−O	176	178	170	**172**			
e_g	rocking; Mo−Mo−O bending	224	226	219	**222**	195		
a_{2u}		248	251	237	**239**	215		
b_{1u}	O−Mo−O bending	291	294	280	**283**	293		
e_g		328	332	318	**322**	302		
b_{1g}	Mo−O stretching	382	390	360	**367**	350	350 (R)	ν_s(Mo−O)
a_{1g}		395	402	367	**373**	371	370 (R)	ν_s(Mo−O)
e_u		412	417	391	**397**	393		
a_{2g}	out-of-plane O−C−O/CH rocking	330	332	340	**340**	333		
b_{2g}		417	421	418	**421**			
e_u		472	479	460	**465**		445 (IR)	ν_{as}(Mo−O)
a_{1g}	**Mo−Mo stretching**	472	482	446	***456***	***406***	***406*** (R)	ν(Mo−Mo)
e_g	Mo−O stretching	456	464	426	**432**	420		
b_{2u}		468	477	445	**452**			
a_{2u}		490	499	463	**471**		470 (IR)	ν_{as}(Mo−O)
e_u	O−C−O bending	750	750	753	**755**		770 (IR)	δ(COO)
b_{1g}		762	763	765	**767**	782	780 (IR)	δ(COO)
a_{1g}		774	776	775	**777**	795	797 (R)	δ(COO)
b_{2g}	CH rocking (out-of-plane	1014	1017	996	**999**			
a_{2g}	O−CH−O deformation)	1018	1021	998	**1001**			
e_u		1020	1023	1000	**1003**		1010 (IR)	π(HCO)
b_{1g}	O−C stretching (sym)	1276	1286	1294	**1306**			
e_u		1279	1289	1298	**1309**		1322 (IR)	ν_s(COO)
a_{1g}		1290	1300	1308	**1319**	1325	1326 (R)	ν_s(COO)
b_{2u}	H−C−O bending (in-plane)	1366	1371	1353	**1358**		1343 (IR)	δ_{as}(HCO)
a_{2u}		1366	1371	1354	**1359**		1355 (IR)	δ_{as}(HCO)
e_g		1367	1372	1355	**1359**			
e_g	O−C stretching (asym)	1461	1475	1474	**1491**			
b_{2u}		1463	1477	1472	**1489**		1520 (IR)	ν_{as}(COO)
a_{2u}		1467	1482	1475	**1493**		1530 (IR)	ν_{as}(COO)
b_{1g}	C−H stretching	3154	3164	3195	**3209**		2822 (IR)	ν(C−H)
e_u		3155	3165	3196	**3209**		2927 2967 (IR)	ν(C−H)
a_{1g}		3156	3166	3197	**3211**		3040 (IR)	ν(C−H)

[a] See ref 13. [b] See ref 14.

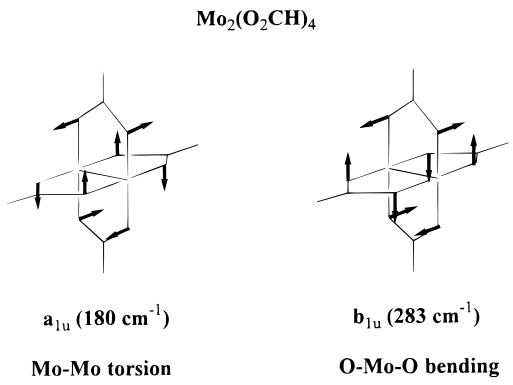

Figure 1. Two fairly localized vibrational modes: an Mo−Mo torsion and one of the O−Mo−O bending vibrations. The lengths of the arrows are proportional to the mass-weighted displacements of the atoms.

Comparison with the experimental data will be made mostly for the blocks as a whole rather than for individual frequencies.

We now look in more detail at the results in Table 3, starting from the block of highest frequencies. The highest bands observed in the IR spectrum, in the region of about 2800−3000 cm^{-1}, were all assigned to C−H stretching vibrations, ν(C−H), even though only one such mode (of e_u symmetry) is expected to be IR active. The calculated ν(C−H) vibrations are all at about 3200 cm^{-1}, that is, about 6−13% higher. The fundamental frequencies in the IR/Raman spectra in the 770−1530 region are all accurately predicted by the DFT calculations, as can be seen by comparing the corresponding blocks by calculations and by experiments in that portion of Table 3.

There should be six normal modes of a_{2u}, b_{2u}, e_g, a_{1g}, b_{1g}, and e_u symmetries in the $Mo_2(O_2CH)_4$ molecule of D_{4h} symmetry that can be assigned to Mo−O stretching vibrations.[15] One set of three such modes, namely, e_g, b_{2u}, and a_{2u}, are calculated at 432, 452, and 471 cm^{-1}, respectively. The Raman band at 420 cm^{-1} may be reasonably assigned to the e_g mode. There are also two IR bands, 445 and 470 cm^{-1}, in this region, both of which had been assigned to ν(Mo−O). The one at 470 cm^{-1} agrees well with the a_{2u} mode for ν(Mo−O) from the calculation. We prefer to assign the IR band at 445 cm^{-1} to the calculated e_u mode at 465 cm^{-1} corresponding to a coupled out-of-plane O−C−O and CH_3 rocking vibration, instead of matching it to the b_{2u} mode at 452 cm^{-1} for ν(Mo−O) since a b_{2u} normal mode is both IR- and Raman-inactive.[15]

Another set of normal modes associated with ν(Mo−O) occurs at lower frequencies according to our calculations. This set comprises the b_{1g}, a_{1g}, and e_u modes at 367, 373, and 397 cm^{-1}, respectively. The bands at 350 and 371 cm^{-1} and at 350 and 370 cm^{-1} in the two Raman spectra, respectively, can be clearly assigned to the b_{1g} and a_{1g} modes. The band at 393 cm^{-1}, on the other hand, is very close to the value at 397 cm^{-1} of the e_u mode but far from any other calculated values and, therefore, is assigned accordingly, even though this may not be an assignment favored by symmetry arguments.

As shown in Figure 2, the totally symmetric a_{1g} normal

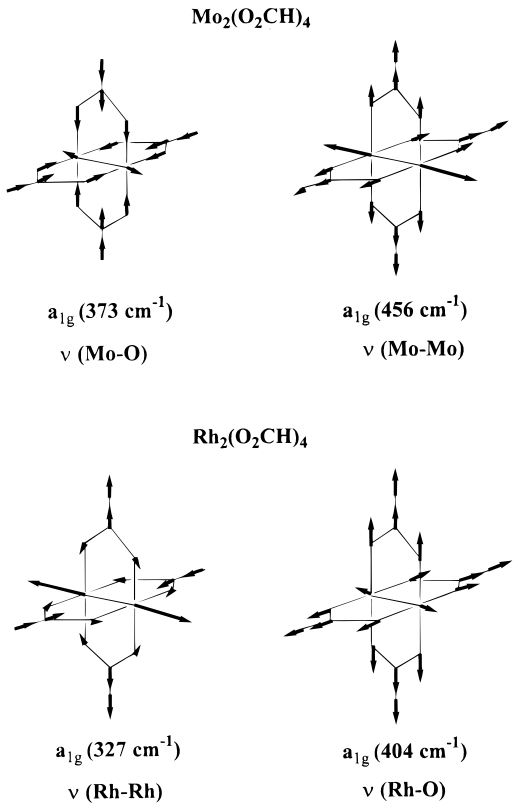

Figure 2. The coupling of M−O and M−M stretching motions in $Mo_2(O_2CH)_4$ and $Rh_2(O_2CH)_4$. The lengths of the arrows are proportional to the mass-weighted displacements of the atoms.

vibration calculated to occur at 456 cm^{-1} may be best described as the Mo−Mo stretching vibration. The calculated frequencies by all DFT methods for this mode (see also Table 3) have a relatively large discrepancy of over 10% when compared with the measured frequency assigned to ν(Mo−Mo) at 406 cm^{-1}. We believe that we should be able to reduce the discrepancy by employing more extended basis functions in the calculations. The calculated values below 330 cm^{-1} mostly compare well with the observed bands in the Raman spectrum even though the assignments are not always guided by the symmetry requirements. The two lowest frequencies, 84 and 95 cm^{-1}, in one[13] of the Raman spectra are left in Table 3 without matching to any calculated values. Considering the overall quality of the calculated results, we think that they might not arise from vibrations of the molecule but are instead lattice modes of the crystal.

It is remarkable that in Table 3 for each block of observed frequencies one can find a matching block from the calculations and that the values in the two blocks are very comparable. It is also interesting to see confirmation of most of the orignal assignments of the IR/Raman spectra. In other words, we may conclude that the measured fundamental frequencies in the IR/Raman spectra of $Mo_2(O_2CH)_4$ can be reproduced by the DFT calculations on the basis of a harmonic model. DFT methods have been known to be successful in reproducing fundamental frequencies for small molecules.[5] We have now shown that this is also true for large transition-metal compounds containing metal−metal bonds.

Vibrational Spectra of $Rh_2(O_2CH)_4$ and $Rh_2(O_2CH)_4(H_2O)_4$. The results of the frequency calculations for the rhodium formate compounds are shown in Tables 4 and 5. Table 4 contains the calculated frequencies above 500 cm^{-1} for the two compounds, and Table 5 is a collection of lower frequencies. There exist only very limited experimental data from an IR spectrum[14] for $Rh_2(O_2CH)_4(H_2O)_4$, which have also been included in the tables. Again, there are no significant differences among the results of the calculations with different DFT methods in different basis sets for either compound. We will then, as before, use the results obtained by the B3PW91 method in the LARGE basis for discussion (see bold-faced columns in both Tables 4 and 5).

In Table 4, the molecular vibrations in $Rh_2(O_2CH)_4$ at frequencies above 700 cm^{-1} are very similar to those calculated for $Mo_2(O_2CH)_4$ except for small numerical differences. This is easily seen by comparing the right side of Table 4 to the lower part of Table 3. It is also clear in Table 4 that adding axial water molecules has little influence on the molecular vibrations in $Rh_2(O_2CH)_4$ in this frequency region. In fact, vibrational couplings between H_2O and $Rh_2(O_2CH)_4$ are negligible as indicated by the calculated nuclear displacements corresponding to the normal nodes in the region.

At the lower frequencies (Table 5), the properties of nuclear motions that may be best described as Rh−O(equatorial) stretching, ν(Rh−O), are still comparable between $Rh_2(O_2CH)_4$ and $Rh_2(O_2CH)_4(H_2O)_2$ and similar to the results for $Mo_2(O_2CH)_4$. Quantitatively, the ν(Rh−O) modes in $Rh_2(O_2CH)_4$ are higher on average than are the same vibrations in the hydrated compound. For $Rh_2(O_2CH)_4$, the normal mode of a_{1g} symmetry at 327 cm^{-1} is surely the one most closely corresponding to a Rh−Rh stretching vibration, ν(Rh−Rh), which is shown in Figure 2 and may be compared to ν(Mo−Mo). In the hydrated compound, however, the situation for Rh−Rh stretching is considerably different. The Rh−Rh stretching vibration is strongly coupled with the Rh−water stretching and, as a result, the normal mode that may be best identified as ν(Rh−Rh) has shifted to higher frequency at 355 cm^{-1}. The coupling can be clearly seen in Figure 3, where axial nuclear displacements in the two relevant normal modes of a_g symmetry are shown. In these two vibrations, the motions of all other nuclei are insignificant and, therefore, neglected for clarity.

One of the major results of this work is that for both of the rhodium formate compounds the vibration best identified as ν(Rh−Rh) has a frequency above 300 cm^{-1}, and as will be seen later, this is also true for dirhodium tetraacetate. These findings owe their importance to the role played by ν(Rh−Rh) in an earlier controversy about the assignment of the electronic spectra of $Rh_2(O_2CR)_4$ compounds. For a succinct but complete review of this problem, a paper by Trexler, Schreiner, and Cotton[16] should be consulted. In a nutshell, the assignment that is supported by much evidence and especially favored by MCD results[16] requires that ν(Rh−Rh) be assigned a frequency at or above 300 cm^{-1}, whereas an alternate assignment would suggest a much lower value (<200 cm^{-1}), with all frequencies in the 300−500 cm^{-1} range having other assignments such as ν(Rh−O) and intraligand vibrations. The results presented here further show that it is necessary to assign the ν(Rh−Rh) vibration to be at 300 cm^{-1} or even higher, which is consistent with the assignments by Clark and co-workers based on their experimental measurements.[17]

We now finish the current section by commenting on the difference in the calculated frequencies for the a_{1u} normal modes corresponding to metal−metal torsional vibration in $Mo_2(O_2CH)_4$ and $Rh_2(O_2CH)_4$. The frequency (180 cm^{-1}) in $Mo_2(O_2$-

(16) Trexler, J. W., Jr.; Schreiner, A. F.; Cotton, F. A. *Inorg. Chem.* **1988**, *27*, 3265.

(17) (a) Clark, R. J. H.; Hempleman, A. J. *Croat. Chem. Acta* **1988**, *61*, 313. (b) Clark, R. J. H.; Hempleman, A. J.; Flint, C. D. *J. Am. Chem. Soc.* **1986**, *108*, 518.

Table 4. Calculated Vibrational Spectra for $Rh_2(O_2CH)_4(H_2O)_2$ and $Rh_2(O_2CH)_4$ at Higher Frequencies (cm^{-1})

	$Rh_2(O_2CH)_4(H_2O)_2$					$Rh_2(O_2CH)_4$			
	3-21G	LARGE				LARGE		3-21G	
C_{2h}	B3PW91	B3LYP	B3PW91	exptl[a]	normal modes	B3PW91	B3LYP	B3PW91	D_{4h}
b_u	605	495	**501**		OH_2 rocking				
a_g	616	498	**503**						
a_u	613	566	**576**						
b_g	612	568	**578**						
a_u	759	756	**759**		O−C−O bending	**753**	749	753	e_u
b_u	759	756	**760**	792		**786**	781	789	b_{1g}
b_g	787	781	**785**			**795**	790	798	a_{1g}
a_g	799	791	**796**						
a_g	1049	1026	**1029**		CH rocking (out-of plane	**1031**	1027	1050	a_{2g}
b_g	1048	1026	**1029**		O−CH−O deformation)	**1031**	1028	1051	b_{2g}
b_u	1051	1028	**1032**	1039		**1033**	1030	1053	e_u
a_u	1051	1028	**1032**	1050					
b_g	1304	1307	**1318**		O−C stretching (sym)	**1323**	1311	1307	e_u
a_u	1304	1308	**1319**	1319		**1323**	1311	1308	b_{1g}
b_u	1305	1308	**1320**	1343		**1331**	1319	1306	a_{1g}
a_g	1311	1315	**1326**						
a_u	1413	1401	**1402**	1379	H−C−O bending (in-plane)	**1394**	1392	1406	e_g
b_g	1414	1400	**1403**			**1394**	1392	1407	b_{2u}
a_g	1414	1400	**1403**			**1396**	1396	1409	a_{2u}
b_u	1415	1403	**1405**	1386					
b_g	1498	1496	**1518**	1533	O−C stretching (asym)	**1496**	1475	1476	e_g
a_g	1499	1497	**1518**			**1532**	1511	1521	b_{2u}
a_u	1535	1525	**1547**	1544		**1593**	1570	1579	a_{2u}
b_u	1591	1582	**1605**	1600					
a_g	1673	1622	**1626**		OH_2 bending				
b_u	1673	1622	**1627**						
b_g	3103	3127	**3140**		C−H stretching	**3168**	3155	3126	b_{1g}
a_u	3103	3128	**3141**	2850		**3189**	3155	3127	e_u
b_u	3103	3128	**3141**	2870		**3170**	3156	3128	a_{1g}
a_g	3105	3129	**3143**						
b_u	3500	3630	**3667**	3440	O−H stretching				
a_g	3501	3631	**3668**	3555					
b_g	3621	3780	**3821**						
a_u	3621	3780	**3821**						

[a] See ref 14.

$CH)_4$ is twice as high as that (90 cm^{-1}) in $Rh_2(O_2CH)_4$. As can be seen in Figure 1, such a torsional motion about the metal−metal bond causes a change in molecular structure from an eclipsed conformation toward a staggered one. Such a motion should be more difficult in $Mo_2(O_2CH)_4$ because there is a Mo−Mo δ bond of full strength which would result the conformational change, whereas there is no δ bond in the corresponding rhodium compound.

B. The Acetate Compounds Molecular Structures. We now turn to the acetate compounds, $Mo_2(O_2CCH_3)_4$ and $Rh_2(O_2CCH_3)_4$. Their optimized molecular structures by various DFT methods and basis sets are displayed in Table 6. The calculations in both cases were carried out by arranging the orientation of the CH_3 groups in such a way that the compounds have C_{4h} symmetry. Once again, as would be expected, the known X-ray structure[18] of the molybdenum compound is excellently reproduced. The molecular structure of the dirhodium acetate compound without any axial ligands has not been experimentally established. Considering the overall excellent performance of DFT methods in geometry optimization for similar compounds in this work and in previous work,[2] the calculated structure for $Rh_2(O_2CCH_3)_4$ ought to be accurate enough to represent the real structure of the compound. It agrees well with the $Rh_2(O_2CCH_3)_4$ portions of $Rh_2(O_2CCH_3)_4L_2$ compounds.

Vibrational Spectrum of $Mo_2(O_2CCH_3)_4$. Vibrational frequencies for this compound were calculated in C_{4h} symmetry by using the optimized geometry and with different DFT methods and basis sets. For convenience of discussion, the results are reported again in two tables which were obtained by the B3PW91 method in both 3-21G and LARGE basis sets. Tables 7 and 8 contain the results at higher and lower frequencies, respectively. As before, blocks are formed in each table to assist comparison with experimental results. The calculated frequencies with the LARGE basis set are to be compared with the reported IR and Raman spectra for $Mo_2(O_2CCH_3)_4$ together with a detailed analysis by Clark and coworkers.[15] The experimental data are also listed in Tables 7 and 8.

Let us first look at Table 7 for the calculated and measured vibrations at frequencies above 650 cm^{-1}. According to the calculations, the normal vibrations of highest frequencies in these molecules should be those of C−H stretching, ν(C−H), in CH_3 at about 3000 cm^{-1}. This is confirmed by the Raman and IR spectra in which a number of weak bands were observed and assigned to ν(C−H) modes (see the block at the bottom of Table 7). The next block of calculated frequencies, in the 1430−1530 cm^{-1} region, corresponds to normal vibrations where the characters of bending in CH_3 and O−C stretching in the O−C−O fragments are strongly coupled. Many observed bands in this similar region had been assigned to the same normal vibrations, while there were still quite a few bands not assigned. With the calculated results, one now may be able to attribute them to molecular vibrations of the same origins as those already assigned. In the next three blocks, the calculated

(18) Cotton, F. A.; Mester, Z. C.; Webb, T. R. *Acta Crystallogr.* **1974**, *B30*, 2768.

Table 5. Calculated Vibrational Spectra for $Rh_2(O_2CH)_4(H_2O)_2$ and $Rh_2(O_2CH)_4$ at Lower Frequencies (cm^{-1})

	$Rh_2(O_2CH)_4(H_2O)_2$					$Rh_2(O_2CH)_4$			
	3-21G	LARGE				LARGE		3-21G	
C_{2h}	B3PW91	B3LYP	B3PW91	exptl[a]	normal modes	B3PW91	B3LYP	B3PW91	D_{4h}
a_u	62	65	**66**		Rh−Rh torsion	**90**	93	70	a_{1u}
b_u	82	58	**63**		H_2O rocking				
a_u	80	73	**77**						
a_g	104	75	**81**						
b_g	94	83	**88**						
a_u	142	125	**124**						
b_g	159	133	**131**						
a_g	121	123	**123**		O−Rh−O bending/out-of-plane	**133**	133	128	b_{2g}
b_u	144	142	**144**		C−H rocking	**153**	152	151	e_u
a_u	168	143	**145**						
a_g	159	156	**157**		in-plane C−H/O−C−O rocking,	**158**	158	155	e_g
b_g	216	158	**159**		Rh−Rh−O bending	**178**	174	183	b_{2u}
a_u	230	166	**169**	168		**249**	245	259	a_{2u}
b_u	219	203	**207**						
b_u	204	200	**202**		O−Rh−O bending/out-of-plane	**222**	221	215	b_{1u}
a_g	265	250	**254**		C−H rocking	**267**	264	266	e_g
b_g	266	252	**255**						
a_g	258	247	**251**		$Rh-OH_2$ stretching				
b_u	306	291	**296**		$Rh-OH_2$ stretching/Rh−Rh−O bending				
a_g	367	348	***355***		*Rh−Rh stretching/Rh−OH_2 stretching*	***327***	319	337	a_{1g}
b_g	286	290	**292**		out-of-plane O−C−O/C−H rocking	**308**	306	299	a_{2g}
b_u	373	360	**366**			**379**	374	375	b_{2g}
a_g	365	362	**367**			**381**	375	385	e_u
a_u	373	361	**367**						
b_g	406	370	**380**		Rh−O stretching	**394**	386	417	b_{1g}
a_g	419	384	**392**			**404**	398	429	a_{1g}
b_g	460	413	**424**			**432**	424	460	e_g
a_g	462	416	**426**						
a_u	465	430	**438**			**461**	453	488	e_u
b_u	471	429	**439**						
a_u	474	439	**447**	455		**460**	454	480	b_{2u}
b_u	482	449	**456**	460		**470**	464	490	a_{2u}

[a] See ref 14.

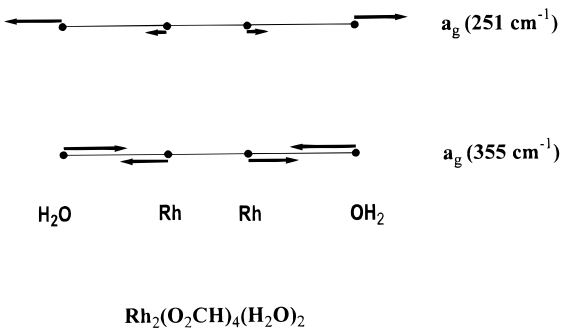

Figure 3. Rh−Rh and $Rh-OH_2$ stretching vibrations in $Rh_2(O_2CH)_4(H_2O)_2$. The lengths of the arrows are proportional to the mass-weighted displacements of the atoms.

and experimental values for $\rho(CH_3)$, ν(C−C), and δ(OCO) are all in excellent agreement.

It is important to point out that in the measured IR spectrum there are also several very weak and broad bands in the region between 1600 and 2500 cm^{-1}.[15] These bands had been given assignments as overtones or combinations bands and are not listed in Table 7. Such assignments are fully supported by the DFT calculations which did not produce any fundamental frequencies in that region.

Comparison of the calculated and observed spectra in the lower frequency region in Table 8, however, is not as straightforward as what we have seen in the previous discussion. We start again from the bottom of Table 8. In the region about 600 cm^{-1}, the calculated a_g mode at 601 cm^{-1} could be inactive since it correlates to an a_{2g} mode in a D_{4h} $M_2(O_2CCH_3)_4$ species. Therefore, the Raman band at 633 may correspond to the calculated b_g mode at 615 cm^{-1}. The two IR bands at 628 and 636 cm^{-1}, on the other hand, may be assigned to the e_u mode which is IR active and calculated at 619 cm^{-1}. The calculations and the experiments agree on the assignments of these normal vibrations, namely, out-of-plane rocking of the OCO groups coupled with the same motion of the CH_3 groups.

In the next block, the calculated e_g, b_u, and a_u normal modes, at 564, 573, and 581 cm^{-1}, respectively, are all corresponding to Mo−O stretching vibrations, ν(Mo−O). They directly correlate to the same type of normal vibrations in the formate compound which occur at 432 (e_g), 452 (b_{2u}), and 471 (a_{2u}) cm^{-1} (see also Table 3). These vibrations, therefore, have shifted over 100 cm^{-1} to higher frequency from $Mo_2(O_2CH)_4$ to $Mo_2(O_2CCH_3)_4$ according to our calculations. Shown in Figure 4, as an example, is a comparison between the b_u normal vibration in the acetate compound and the corresponding b_{2u} vibration in the formate compound.

The calculated values in this region have an excellent match to those observed in the Raman (569 and 573 cm^{-1}) and IR (575 and 583 cm^{-1}) spectra. The measured data, however, had all been assigned to in-plane rocking of the O−C−O groups by analogy to the spectra of $Na(O_2CCH_3)$.[15] Using the calculated results, we may reassign the Raman bands at 569 and 573 cm^{-1} to be ν(Mo−O) of e_u symmetry calculated at 564 cm^{-1}, and the two IR bands (575 and 583 cm^{-1}) to the same type of vibration but of b_u and a_u symmetries which are calculated at 573 and 581 cm^{-1}, respectively. The different assignments are indicated in Table 8 by italics.

The normal mode of a_g symmetry calculated at 453 cm^{-1}

Table 6. Results of Geometry Optimization for the Acetate Compounds $M_2(O_2CCH_3)_4$ (M = Mo, Rh)

$Mo_2(O_2CCH_3)_4$					$Rh_2(O_2CCH_3)_4$		
	3-21G	LARGE				3-21G	LARGE
	B3PW91	B3LYP	B3PW91	exptl[a]		B3LYP	B3PW91
			distance (Å)				
Mo−Mo	2.089	2.122	2.108	2.0934(8)	Rh−Rh	2.388	2.394
Mo−O	2.091	2.132	2.119	2.119(4)	Rh−O	2.061	2.067
O−C	1.299	1.301	1.299	1.277(7)	O−C	1.296	1.294
C−C	1.499	1.497	1.492	1.501(9)	C−C	1.511	1.497
C−H	1.098 1.092	1.097 1.091	1.097 1.091		C−H	1.097 1.091	1.096 1.091
			angle (deg)				
Mo−Mo−O	92.23	91.74	91.87	91.8(1)	Rh−Rh−O	88.71	88.56
Mo−O−C	117.70	118.37	118.22	117.5(4)	Mo−O−C	118.95	119.23
O−Mo−O	89.91	89.95	89.94	89.9(2)	O−Rh−O	89.97	89.96
O−C−O	120.14	119.78	119.81	121.3(6)	O−C−O	124.67	124.42

[a] Average bond distances and angles from crystal structure data of $Mo_2(O_2CCH_3)_4$ (see ref 18).

Table 7. Calculated and Measured Vibrational Spectra for $Mo_2(O_2CCH_3)_4$ at Higher Frequencies (cm^{-1}) by B3PW91 Method

calcd				exptl[a]			
sym	3-21G	LARGE	normal modes	Raman	assignment	IR	assignment
e_u	660	**663**	O−C−O bending/C−C stretching	686	δ(OCO)	676	δ(OCO)
b_g	670	**674**		692	δ(OCO)		
a_g	686	**687**		706	δ(OCO)		
e_u	918	**947**	C−C stretching/O−C−O bending				
b_g	923	**951**		944	ν(C−C)		
a_g	927	**954**		945	ν(C−C)	973	ν(C−C)
a_u	1061	**1060**	H rocking in CH_3	1036	$\rho(CH_3)$	1034	$\rho(CH_3)$
e_g	1062	**1061**		1047	$\rho(CH_3)$	1046	$\rho(CH_3)$
b_u	1063	**1062**		1058	$\rho(CH_3)$	1054	$\rho(CH_3)$
a_g	1097	**1096**					
e_u	1098	**1097**					
b_g	1098	**1097**					
b_g	1406	**1433**	CH_3 bending/O−C−O stretching (sym)	1355	$\delta_{sym}(CH_3)$	1352	$\delta_{sym}(CH_3)$
e_u	1411	**1435**		1367	$\delta_{sym}(CH_3)$	1355	$\delta_{sym}(CH_3)$
a_g	1424	**1440**		1403	$\delta_{asym}(CH_3)$	1407	$\delta_{asym}(CH_3)$
b_u	1437	**1453**	CH_3 bending/O−C−O stretching (asym)	1422	ν_{sym}(COO)	1420	
a_u	1441	**1455**		1431	$\delta_{asym}(CH_3)$	1431	$\delta_{asym}(CH_3)$
e_g	1437	**1456**		1440		1440	ν_{sym}(COO)
b_g	1443	**1458**	O−C−O stretcing/CH_3 bending (sym)	1443		1451	$\delta_{asym}(CH_3)$
e_u	1443	**1461**		1460	$\delta_{asym}(CH_3)$	1454	
a_g	1444	**1469**		1500	ν_{asym}(COO)	1475	ν_{aasym}(COO)
b_g	1534	**1518**				1500	
e_u	1535	**1519**				1514	
a_g	1535	**1519**				1520	
a_u	1543	**1529**	O−C−O stretching/CH_3 bending (asym)			1524	
b_u	1543	**1530**				1531	
e_g	1542	**1530**					
b_g	3067	**3073**	C−H stretching	2931	ν(C−H)	2931	ν(C−H)
e_u	3067	**3073**		2942	ν(C−H)	2975	ν(C−H)
a_g	3067	**3074**		2977	ν(C−H)	3007	ν(C−H)
a_g	3145	**3159**		3007	ν(C−H)	3017	ν(C−H)
e_u	3145	**3159**		3018	ν(C−H)		
b_g	3145	**3159**					
b_u	3191	**3203**					
e_g	3191	**3203**					
a_u	3191	**3203**					

[a] See ref 15.

corresponds to the Mo−Mo stretching vibration. It is shown in Figure 5, which may be compared to ν(Mo−Mo) in the corresponding formate compound in Figure 2. It is interesting to note that both calculated and measured frequencies for the Mo−Mo stretching vibration in the acetate compound, 453 and 404 cm^{-1}, respectively, are essentially the same as those in the formate compound, 456 and 406 cm^{-1}, respectively. Again, we see that the calculated value is over 10% higher than that determined by the Raman spectrum.

The next calculated block toward lower frequencies contains another set of ν(Mo−O) modes of b_g, a_g, and e_u symmetries at 314, 323, and 377 cm^{-1}, respectively. These normal vibrations are very similar to the set of b_{1g}, a_{1g}, and e_u ν(Mo−O) modes in the formate compound that are calculated 367, 373, and 397 cm^{-1}, respectively, (see also Table 3). As shown in Table 8, there are four Raman bands and four IR bands observed in the 300−373 cm^{-1} region that had been all assigned to ν(Mo−O). We agree with the assignment for the Raman bands at 315 and 323 cm^{-1} and further assign them to the calculated b_g and a_g modes, respectively. The same is true for the IR bands at 353 and 373 cm^{-1}, which we think may belong to the e_u modes. However, we propose that the Raman bands at 301 and 306 cm^{-1} be assigned to the calculated e_g mode of O−Mo−O bending at at 326 cm^{-1} and the IR bands at 311 and 342 cm^{-1} to the in-plane rocking modes of b_u and a_u symmetries, calculated at 296 and 331 cm^{-1}, respectively.

In the region below 300 cm^{-1}, a few bands that were originally given tentative assignments as CH_3 torsion,[15] $\tau(CH_3)$,

Table 8. Calculated and Measured Vibrational Spectra for $Mo_2(O_2CCH_3)_4$ at Lower Frequencies (cm^{-1}) by B3PW91 Method

calcd				exptl[a]					
sym	3-21G	LARGE	normal modes	Raman		assignment	IR		assignment
b_u	39	**30**	CH_3 torsion						
a_u	39	**31**							
e_g	39	**31**							
e_u	59	**60**	out-of-plane CH_3/O−C−O rocking	65	72				
b_g	62	**64**		83					
a_g	131	**135**		143		*τ(CH₃)*	146		
b_u	126	**123**	*b*	106			91		
a_u	174	**169**	*b*				183		*τ(CH₃)*
a_u	177	**177**	Mo−Mo torsion						
e_g	215	**210**	*b*	190	204	*δ(Mo−Mo−O)/ δ(O−Mo−O)*			
b_g	233	**227**	O−Mo−O bending/CH_3	220		*τ(CH₃)*	230	235	*δ*(Mo−Mo−O)/ *δ*(O−Mo−O)
e_u	251	**242**	out-of-plane rocking						
e_g	273	**272**	*b*						
b_u	295	**283**	O−Mo−O bending						
b_u	296	**296**	*b*				311		*ν(Mo−O)*
e_g	338	**326**	O−Mo−O bending	*301*	*306*	*ν(Mo−O)*			
a_u	336	**331**	*b*				342		*ν(Mo−O)*
b_g	330	**314**	Mo−O stretching	315		*ν*(Mo−O)			
a_g	341	**323**		323		*ν*(Mo−O)			
e_u	398	**377**					353	373	*ν*(Mo−O)
a_g	481	**453**	**Mo−Mo stretching**	**404**		***ν*(Mo−Mo)**			
e_g	*579*	***564***	*Mo−O stretching*	*569*	*573*	*in-plane*			
b_u	*583*	**573**				*ρr(COO)*	575		*in-plane*
a_u	*596*	**581**					583		*ρr(COO)*
a_g	607	**601**	out-of-plane O−C−O/CH_3						
b_g	620	**615**	rocking	633	out-of-plane				
e_u	625	**619**			*ρw*(COO)		628	636	out-of-plane *ρw*(COO)

[a] See ref 15. [b] These normal modes of vibration have mixed characters of in-plane O−C−O/CH_3 rocking and Mo−Mo−O bending.

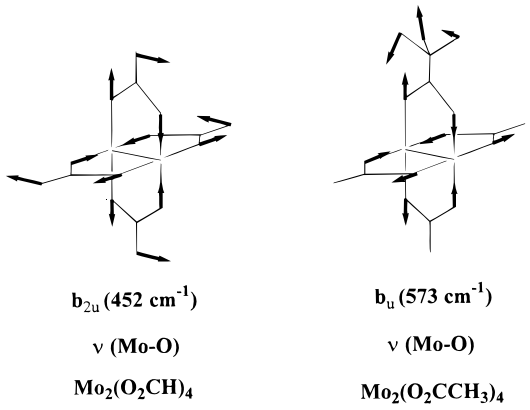

Figure 4. High-frequency Mo−O stretching vibrations in $Mo_2(O_2CH)_4$ and $Mo_2(O_2CCH_3)_4$. The lengths of the arrows are proportional to the mass-weighted displacements of the atoms. Only one CH_3 is shown in $Mo_2(O_2CCH_3)_4$ for clarity.

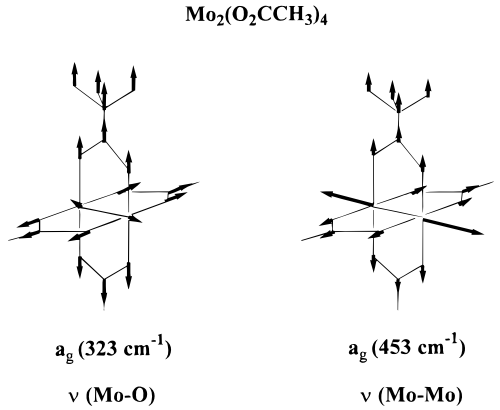

Figure 5. Mo−O and Mo−Mo stretching vibrations in $Mo_2(O_2CCH_3)_4$. The lengths of the arrows are proportional to the mass-weighted displacements of the atoms. Only one CH_3 is shown for clarity.

have been matched to different origins. Our calculations suggest that $\tau(CH_3)$ should occur at a much lower frequency region. In addition, we have matched all of those observed bands below 300 cm^{-1} but without assignments to appropriate normal modes.

Vibrational Spectrum of $Rh_2(O_2CCH_3)_4$. Shown in Tables 9 and 10 are the calculated frequencies and those from Raman and IR spectra[17a] for the rhodium acetate compound. The results at higher frequencies as listed in Table 9 are totally comparable with those in Table 7 for the molybdenum acetate compound. In fact, our previous discussion about Table 7 is essentially all applicable to the results in Table 9 for $Rh_2(O_2CCH_3)_4$. There is only one point to be mentioned before we direct our attention to the results in Table 10. One may notice that there are five bands in the IR spectrum whose assignments are uncertain and were given question marks.[17a] Through comparison with the calculated results, one may assign these bands with confidence to the normal modes corresponding CH_3 bending and/or O−C stretching vibrations, just as were the other observed bands in the frequency region.

At lower frequency (Table 10), the situation is still generally comparable. As in the case of *ν*(Mo−O) in $Mo_2(O_2CCH_3)_4$, the calculated *ν*(Rh−O) at higher frequencies, namely, those at 579 (e_g), 588 (b_u), and 592 (a_u) cm^{-1}, have a good match to the Raman band at 591 cm^{-1} and the IR bands at 602 and 606 cm^{-1} although these had again been previously assigned to in-plane rocking or the O−C−O groups. There is also good agreement between the calculated and measured values for Rh−O stretching vibrations at lower frequencies. Comparison of the remaining results in Table 10 essentially follows what we did for $Mo_2(O_2CCH_3)_4$ in Table 8 and, therefore, need not be repeated. Instead, we will direct the rest of our discussion to the Rh−Rh stretching vibration.

Experimentally, a band at 355 cm^{-1} in the Raman spectrum of $Rh_2(O_2CCH_3)_4$ has been assigned to the Rh−Rh stretching vibration as shown in Table 10. The assignment was based on

Table 9. Calculated and Measured Vibrational Spectra for $Rh_2(O_2CCH_3)_4$ at Higher Frequencies (cm^{-1}) by B3PW91 Method

cakcd			exptl[a]				
sym	LARGE	normal modes	Raman	assignment	IR		assignment
e_u	689	O−C−O bending/C−C stretching			700	704	δ(OCO)
b_g	714				709		δ(OCO)
a_g	720		734	δ(OCO)	722		
e_u	946	C−C stretching/O−C−O bending			941	945	ν(CC)
b_g	955		954	ν(CC)			
a_g	958		962	ν(CC)			
e_g	1066	H rocking in CH_3	1040	$\rho(CH_3)$	1037		$\rho(CH_3)$
b_u	1068		1050	$\rho(CH_3)$	1046		$\rho(CH_3)$
a_u	1069		1058	$\rho(CH_3)$	1051		$\rho(CH_3)$
a_g	1096						
e_u	1098				1252		
b_g	1099				1260		
b_g	1427	O−C−O sym strectching/CH_3 sym bending	1357	$\delta_s(CH_3)$	1352		$\delta_s(CH_3)$
e_u	1428		1368	$\delta_s(CH_3)$	1357		$\delta_s(CH_3)$
a_g	1437		1400	$\delta_{as}(CH_3)$	1372		
b_g	1451		1425	$\delta_{as}(CH_3)$	1405		$\delta_{as}(CH_3)$
e_u	1451		1436	$\delta_{as}(CH_3)$	1415		$\delta_{as}(CH_3)$
a_g	1459		1445	ν(COO)	1423		
e_g	1461	O−C−O asym stretching/CH_3 asym bending	1460	$\delta_{as}(CH_3)$	1429		$\delta_{as}(CH_3)$
b_u	1481		1500		1438		ν_s(COO)
a_u	1496				1446		$\delta_{as}(CH_3)$
b_g	1518	CH_3 sym bending/O−C−O sym stretching			1503		?
e_u	1518				1527		?
a_g	1519				1534		?
e_g	1528	CH_3 asym bending/O−C−O asym stretching			1547		?
b_u	1543				1555		?
a_u	1589				1586		ν_{as}(COO)
b_g	3078	C−H stretching	2938	ν(C−H)	2930		ν(C−H)
e_u	3078		2983	ν(C−H)	2979		ν(C−H)
a_g	3078		3012	ν(C−H)	3014		ν(C−H)
a_g	3164						
e_u	3165						
b_g	3165						
e_g	3205						
b_u	3205						
a_u	3205						

[a] See ref 17a.

Table 10. Calculated and Measured Vibrational Spectra for $Rh_2(O_2CCH_3)_4$ at Lower Frequencies (cm^{-1}) by B3PW91 Method

calcd			exptl[a]				
sym	LARGE	normal modes	Raman	assignment	IR		assignment
b_u	37	CH_3 torsion					
e_g	38						
a_u	39						
b_g	64	CH_3/O−C−O rocking (out-of-plane)	59				
e_u	68						
a_g	127				106		
a_u	83	Rh−Rh torsion	84		93		
b_u	132	*b*	144	*τ(CH₃)*	142		
e_g	154	*b*	176	*δ(Rh−Rh−O)*	163		
a_u	184	CH_3 rocking (in-plane)			209		$\tau(CH_3)$
b_u	222	O−Rh−O bending			214		δ(O−Rh−O)
b_g	222	O−Rh−O bending	188	δ(O−Rh−O)			
e_g	238	*b*	273				
e_u	246	O−Rh−O bending			255	257	
e_g	288	O−Rh−O bending	298	311			
b_u	290	*b*			318		
a_u	319	*b*			*333*		*ν(Rh−O)*
a_g	320	Rh−O stretching	331	ν(Rh−O)			
b_g	326	Rh−O stretching	338	ν(Rh−O)	359		ν(Rh−O)
a_g	**351**	**Rh−Rh stretching**	**355**	**ν(Rh−Rh)**			
e_u	392	Rh−O stretching	389	ν(Rh−O)	383	398	ν(Rh−O)
e_g	579	Rh−O stretching	591	*in plane* ρ_r(COO)			
b_u	588				602		*in-plane* ρ_r*(COO)*
a_u	592				606		*in-plane* ρ_r*(COO)*
a_g	591	O−C−O/CH_3 rocking (out-of-plane)					
b_g	603		629	out-of-plane ρ_w(COO)	621		out-of-plane ρ_w(COO)
e_u	606				635	628	

[a] See ref 17a. [b] These normal modes of vibration have mixed characters of O−C−O and CH_3 in-plane rocking and Mo−Mo−O bending.

a very convincing comparison between the Raman spectra of $Rh_2(O_2CCH_3)_4$ and $Mo_2(O_2CCH_3)_4$.[17a] Our calculations show that, while the a_g normal mode at 351 cm^{-1} may be best described as Rh−Rh stretching the coupling of ν(Rh−Rh) with other normal vibrations in $Rh_2(O_2CCH_3)_4$ is much stronger than in any other compounds we have studied. Such a coupling can

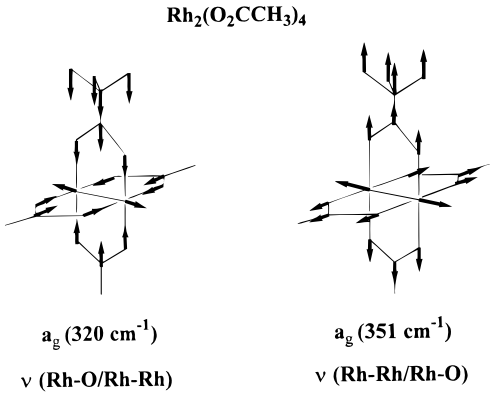

Figure 6. Rh−O and Rh−Rh stretching vibrations in $Rh_2(O_2CCH_3)_4$. The lengths of the arrows are proportional to the mass-weighted displacements of the atoms. Only one CH_3 is shown for clarity.

be seen clearly in Figure 6, where the a_g normal vibration at 351 cm^{-1} is illustrated together with another a_g mode at 320 cm^{-1}. Comparing the normal vibrations in Figure 6 to those in Figures 2 and 5, it is surprising to see how the distribution of the Rh−Rh stretching motion among normal modes could change so much in going from $Rh_2(O_2CH)_4$ to $Rh_2(O_2CCH_3)_4$. There is virtually no difference in the behavior of ν(Mo−Mo) between the formate and acetate compounds of molybdenum. Apart from this surprise, the calculation further confirms that ν(Rh−Rh) can only appear in the region above 300 cm^{-1} in the vibrational spectra of dirhodium compounds of this type.

Conclusions

We show in this work that the methods of density functional theory can be used for calculation of vibrational frequencies of large and complicated transition-metal compounds containing metal−metal bonds of different orders. The calculated frequencies are not only qualitatively but also quantitatively in accord with experimental vibrational spectra. The DFT methods, therefore, are further proven to be a very valuable theoretical tool in the study of metal−metal bonding by correctly predicting an important property of metal−metal bonding, namely, metal−metal stretching frequencies, in addition to the metal−metal bond distances. It is also noted that further investigation is needed to improve the results in the very low-frequency region where high accuracy is essential in order to use the calculations for analysis of experimental spectra.

Acknowledgment. We thank the National Science Foundation for support and the Supercomputing Center and the Department of Chemistry at Texas A&M University for granting computer time. We are grateful to Professor M. B. Hall for computer program access.

JA9738236